Supplement 2

ZIRCON ANALYSIS METHOD DETAILS AND ADDITIONAL RESULTS

Analysis by
Kevin Chamberlain, University of Wyoming, WY, USA
Chris Holm-Denoma, U.S. geological Survey, Denver, CO, USA

METHODS

Zircon Laser Ablation (USGS)

Zircon was ablated with a Photon Machines Excite™ 193 nm ArF excimer laser that was coupled to a Nu Instruments AttoM high-resolution magnetic-sector inductively coupled plasma mass spectrometer in spot mode (150 total bursts for zircon) with a repetition rate of 5 Hz, laser energy of ~3 mJ, and an energy density of 4.11 J/cm2. Pit depths are typically less than 20 µm. The rate of He carrier gas flow from the HelEx cell of the laser was ~0.6 L/min. Make-up Ar gas (~0.2 L/min) was added to the sample stream prior to its introduction into the plasma. Nitrogen with flow rate of 5.5 mL/min was added to the sample stream to allow for significant reduction in ThO+/Th+ (<0.5%) and improved the ionization of refractory Th (Hu et al.,2008). The laser spot sizes for zircon were ~25 µm. With the magnet parked at a constant mass, the flat tops of the isotope peaks of 202 Hg, 204 (Hg+Pb), 206 Pb, 207 Pb, 208 Pb, 232 Th, 235 U, and 238 U were measured by rapidly deflecting the ion beam with a 30 s on-peak background measured prior to each 30s analysis. Raw data were reduced off-line using the Iolite™ 2.5 program (Paton et al., 2011) to subtract on-peak background signals, correct for U-Pb downhole fractionation, and normalize the instrumental mass bias using external mineral reference materials, the ages of which had previously been determined by ID-TIMS. Ages were corrected by standard sample bracketing with the primary zircon reference material Temora2 (417 Ma; Black et al., 2004) and secondary reference material FC-1 (Paces and Miller, 1999), Plešovice (337 Ma, Sláma et al., 2008) and Fish Canyon (Schmitz and Bowring, 2001). Reduced data were compiled into Wetherill concordia diagrams using Isoplot 4.15 (Ludwig, 2012). 206 Pb/ 238 U ages are reported for igneous zircon samples less than ~1300 Ma and 207 Pb/ 206 Pb ages are used for older ages following the recommendations of Gehrels (2012).

Zircon TIMS (University of Wyoming)

Dating efforts by TIMS were focused on euhedral grains with sharp crystal vertices, as these have the best potential to be derived from ash fall and youngest. Morphologies that are diagnostic of volcanic, ash-fall origin include elongate tips and longitudinal bubble tracks and cavities. Sub-populations of these potential 'ash-fall' zircons along with euhedral grains were selected from each sample for annealing and chemical abrasion prior to U-Pb dating by isotope dilution, thermal ionization mass spectrometry of single grains (CA-ID-TIMS) adapted from Mattinson (2005). Selected grains were annealed at 850 °C for 50 hours, then dissolved in two steps. The first step was at 180 °C for 12 hours in hydrofluoric (HF) and nitric (HNO3) acids to remove the most metamict portions of the grains. Single grains were then spiked with a mixed 205Pb-233U-235U tracer (ET535) and dissolved completely at 240 °C in HF and HNO3 acids for 30 hours. Following conversion to chlorides, the samples were loaded in silica gel and phosphoric acid and analyzed in single collector Daly mode on a Micromass S54 TIMS at the University of Wyoming.

ADDITIONAL FIGURES AND RESULTS

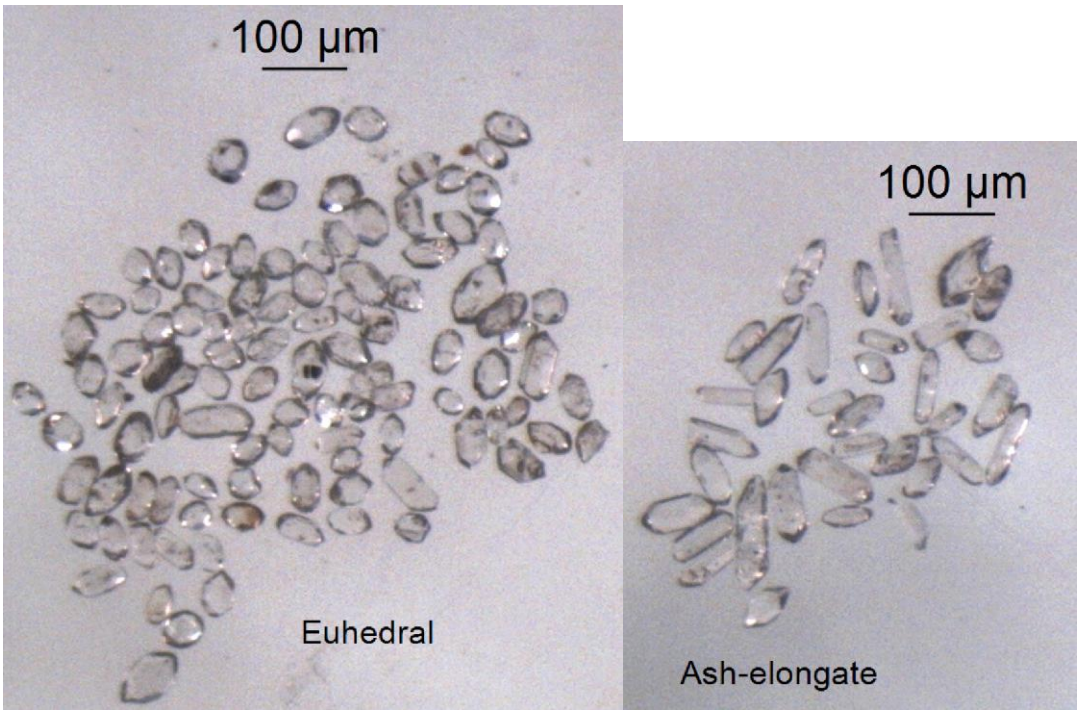

Figure S2-1. Examples of recovered euhedral, short to equant (left) and elongate (right) zircons from tonstein sample RD0814-36. A minor population of rounded, detrital zircons also exists, but was not imaged. Elongate zircons often display characteristics that are typical of ash-fall zircons, although for this sample, the smaller, equant, euhedral zircons yielded the youngest dates (Table 1) and are the best estimates for the timing of ash deposition.

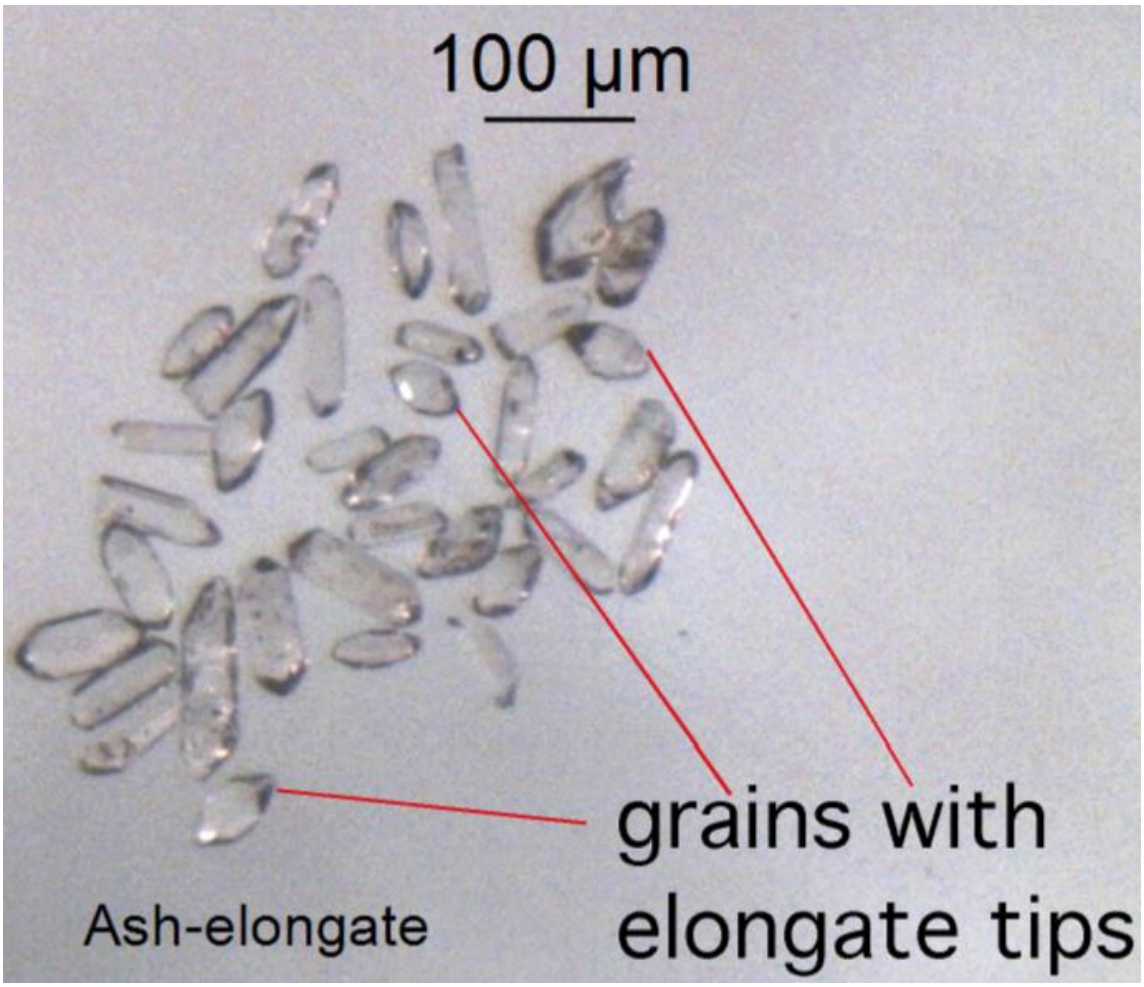

Figure S2-2. Close-up image of elongate and ash-type zircons from RD0814-36. The 3 annotated grains have elongate, sharp tips that are typical of volcanic, ash-fall zircon morphologies. The youngest date from these grains was 55.9±0.7 Ma, which is slightly older than those from the more equant, euhedral sub-population (Figure A1, A4, Table 1).

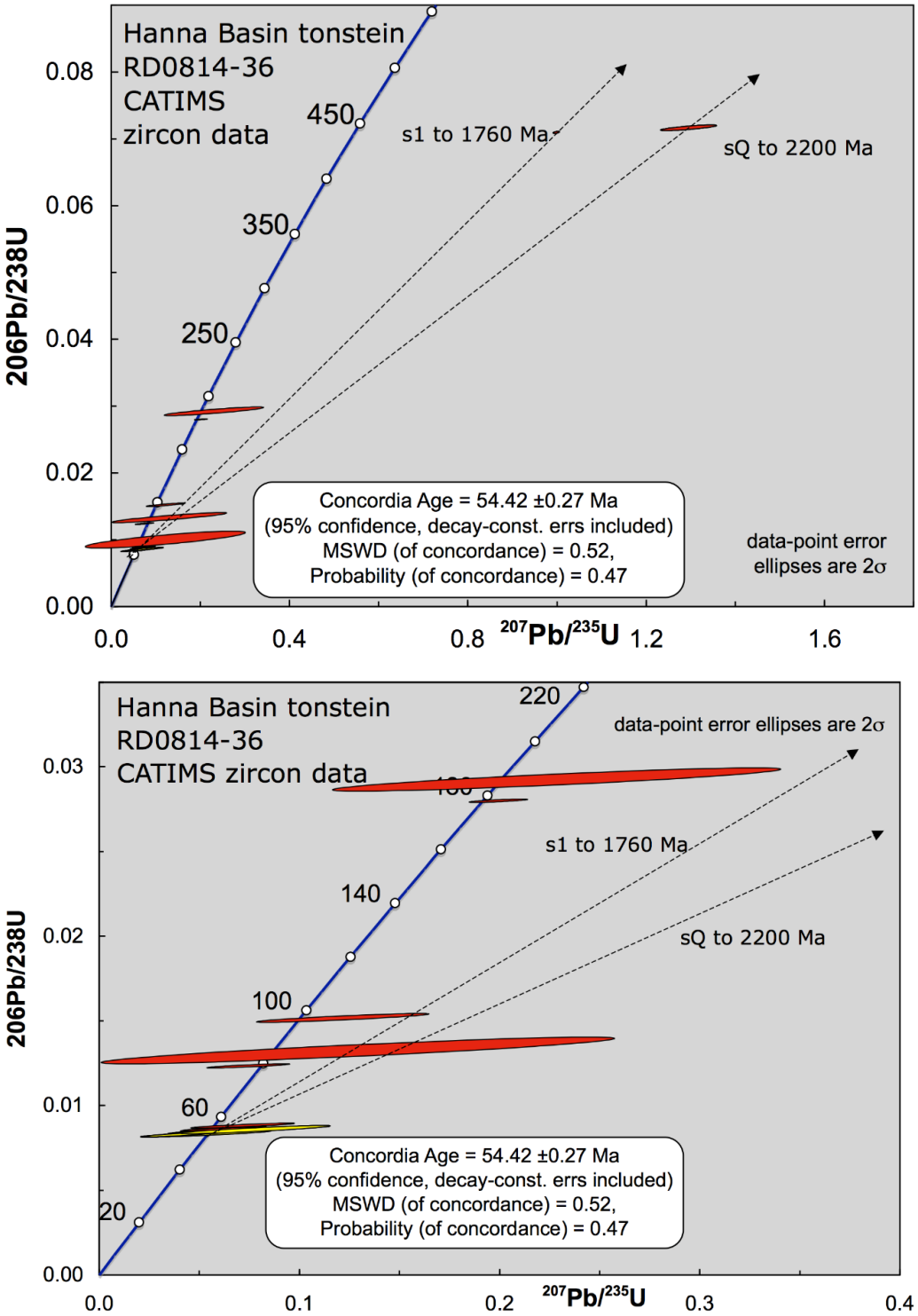

Figure S2-3. Concordia plots of 19 single zircon CATIMS analyses from tonstein RD0814-36. Euhedral zircons yielded dates from 53.9 to 1706 Ma (Table 1). One grain is concordant at 1706 Ma, two grains, s1 and sQ, reflect ca. 54 Ma zircons that contain older cores, ca. 1760 and 2200 Ma. Concordant analyses from 55 to 185 Ma are interpreted as pre-eruptive and inherited/detrital zircons. The best estimate of the eruptive age comes from Concordia Age of the 4 youngest, concordant zircons.

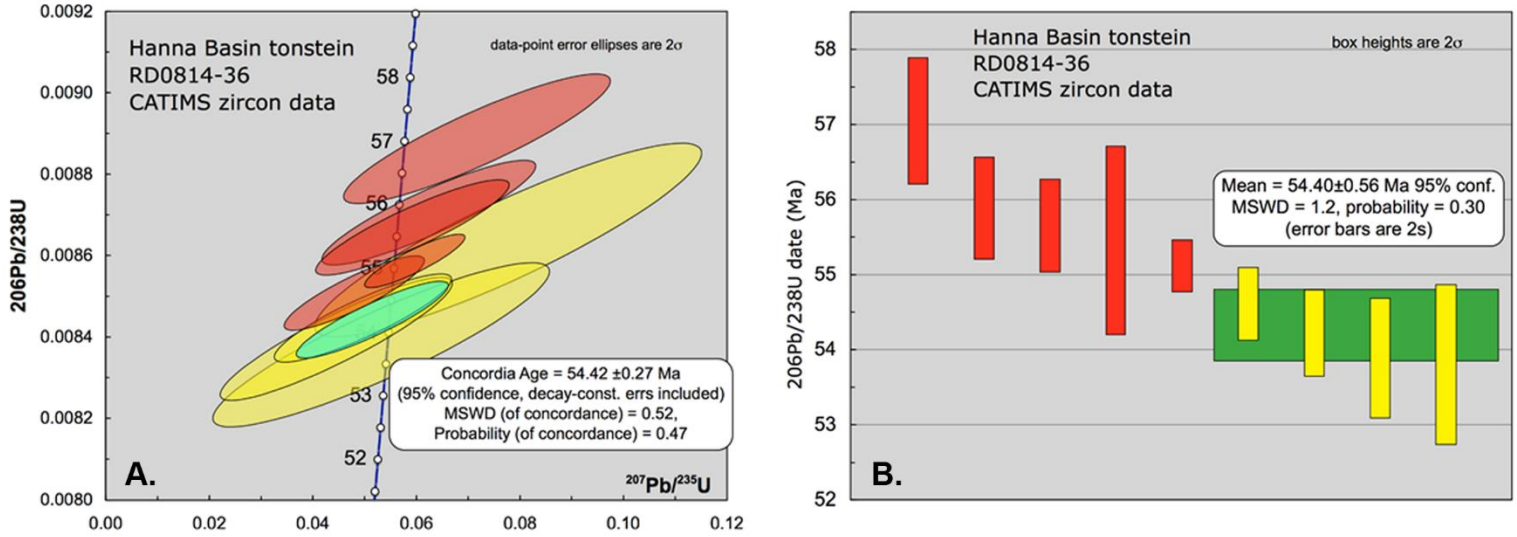

Figure S2-4. **a)** Close-up concordia plot of the youngest nine single grain analyses from RD0814-36. Concordia Age (Ludwig 1998, green ellipse) includes the $^{206}Pb/^{238}U$ and $^{207}Pb/^{235}U$ data, as well as the decay constant errors. The Concordia Age of 54.42±0.27 Ma from the 4 youngest zircons (yellow ellipses) is interpreted as the best estimate of the age of ash deposition in this sample. The older zircons (red ellipses) are interpreted as pre-eruptive, antecrystic zircons from the magma chamber, or slightly older, volcanic zircons entrained during ash-fall deposition. b) Plot of $^{206}Pb/^{238}U$ dates of the 9 youngest zircon analyses from RD0814-36, and weighted mean calculation of the four single-grain analyses of equant zircons (yellow bars). Weighted mean date overlaps with Concordia Age calculation.

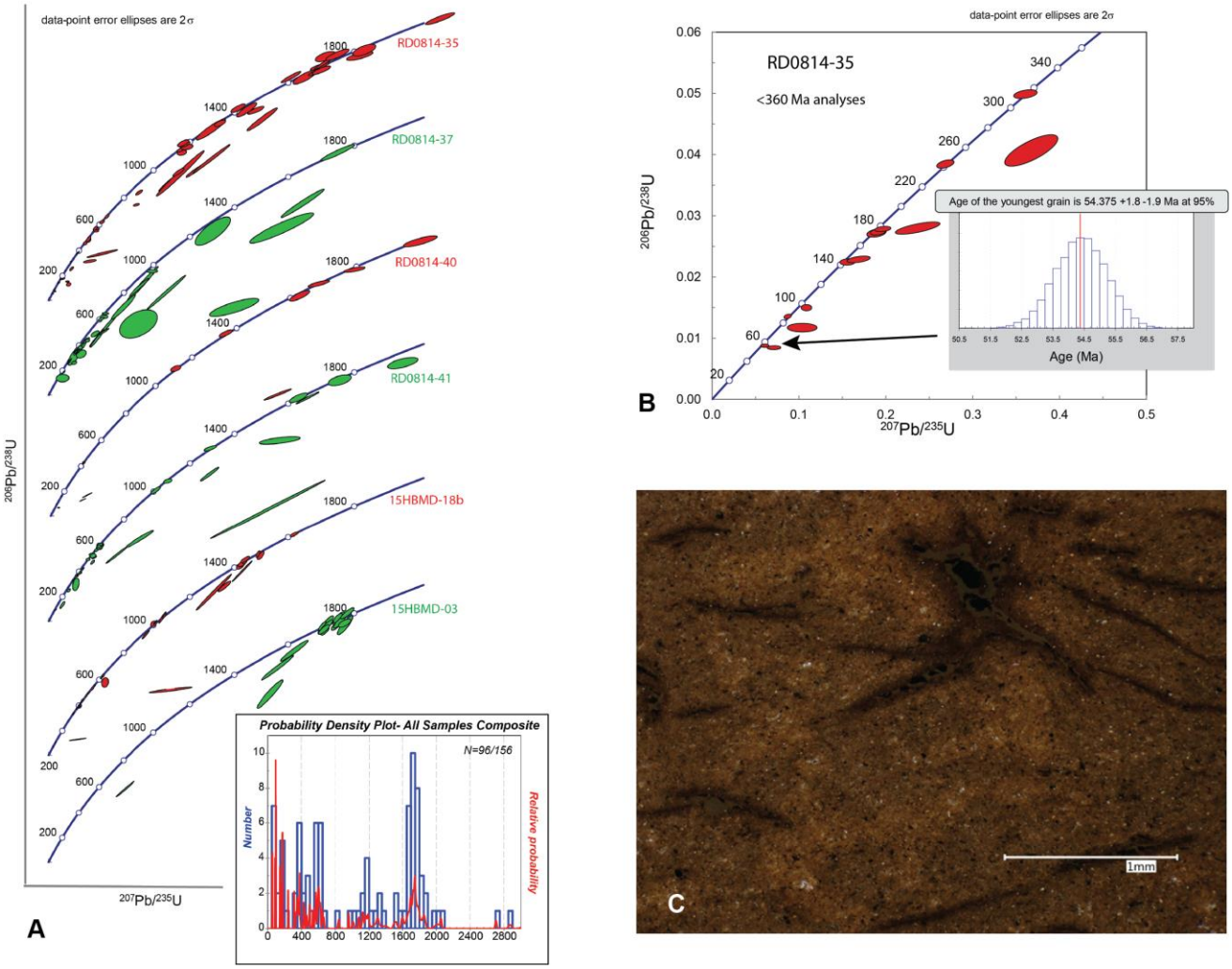

Figure S2-5. A) Hanna Basin Normal Concordia. B) Hanna Basin Normal Youngest. C) Thin section of sample 15HBMD-03, indicating fine-grained nature and coal particles present in “ashy” sample within Coal 84.

Table S2-1 CATIMS U-Pb zircon data

Sample	Weight (µg)	U (ppm)	sample Pb (ppm)	sample Pb (pg)	cPb (pg)	Pb*/Pbc	Th/U	Corrected atomic ratios 206Pb/204Pb	208Pb/206Pb	206Pb/238UTh (rad.)	%err	207Pb/235U (rad.)	%err	207Pb/206PbTh (rad.)	%err	206/238Th Age (Ma)	err	207/235 Age (Ma)	Rho
RD0814-036 volcanic tuff								*54.42±0.27 Ma Concordia Age of 4 youngest grains (MSWD=0.52), plus antecrystic and detrital grains*											
euh sG	0.1	429	3.8	0.5	1.3	0.3	0.24	39	0.08	0.00840	(2.0)	0.0533	(50.0)	0.0460	(48.3)	53.91	±1.06	52.7	0.90
euh H-2gr	0.2	181	1.7	0.4	0.7	0.5	0.49	51	0.13	0.00841	(1.5)	0.0445	(41.2)	0.0384	(39.9)	53.99	±0.79	44.2	0.91
euh sE	0.1	565	4.8	0.6	0.9	0.6	0.19	58	0.06	0.00846	(1.0)	0.0497	(28.2)	0.0426	(27.2)	54.33	±0.57	49.2	0.88
euh sB	0.1	694	6.2	0.7	0.9	0.8	0.39	72	0.11	0.00852	(0.9)	0.0480	(23.1)	0.0408	(22.3)	54.71	±0.48	47.6	0.87
euh sF	0.1	501	4.6	0.6	0.5	1.1	0.30	89	0.10	0.00860	(0.6)	0.0598	(13.3)	0.0504	(12.8)	55.21	±0.34	59.0	0.88
euh sR	0.1	559	5.3	0.6	1.9	0.3	0.35	38	0.15	0.00865	(2.2)	0.0779	(39.3)	0.0653	(37.3)	55.54	±1.25	76.2	0.90
euh sW	0.1	625	5.7	0.7	1.1	0.6	0.34	56	0.12	0.00868	(1.1)	0.0593	(25.9)	0.0495	(24.9)	55.74	±0.61	58.5	0.89
elong sC	1.1	89	0.8	0.9	1.6	0.6	0.36	53	0.13	0.00872	(1.2)	0.0625	(27.0)	0.0520	(26.0)	55.97	±0.67	61.6	0.89
elong sI	0.4	106	1.1	0.5	0.9	0.5	0.57	46	0.23	0.00890	(1.5)	0.0718	(29.4)	0.0585	(28.1)	57.11	±0.84	70.4	0.89
euh sU	0.1	395	49.3	5.9	9.4	0.1	0.29	22	0.17	0.01005	(10.1)	0.1210	(121.2)	0.0873	(112.9)	64.48	±6.52	115.9	0.83
elong sD	1.4	23	0.4	0.5	0.5	1.0	1.46	66	0.43	0.01238	(0.9)	0.0745	(22.7)	0.0436	(21.9)	79.31	±0.72	73.0	0.87
euh sS	0.1	88	1.9	0.2	1.1	0.2	0.98	27	0.46	0.01330	(4.9)	0.1294	(81.1)	0.0706	(76.8)	85.16	±4.16	123.6	0.90
euh sM	0.1	598	11.6	0.8	1.4	0.6	0.93	47	0.36	0.01523	(1.4)	0.1220	(28.9)	0.0581	(27.7)	97.43	±1.41	116.9	0.89
euh sY	0.1	169	5.0	0.7	1.0	0.7	3.36	52	0.46	0.02195	(1.4)	0.0615	(74.3)	0.0203	(73.1)	139.96	±1.91	60.6	0.88
euh sL	0.1	1120	34.4	2.4	0.9	2.6	0.61	171	0.20	0.02800	(0.3)	0.1996	(6.0)	0.0517	(5.8)	178.04	±0.54	184.8	0.78
elong sK	0.3	145	5.4	1.8	4.1	0.4	0.37	40	0.31	0.02924	(1.9)	0.2286	(40.0)	0.0567	(38.3)	185.76	±3.57	209.0	0.88
euh s1	0.2	332	28.1	5.7	0.4	14.6	0.22	798	0.27	0.07100	(0.2)	0.9975	(0.6)	0.1019	(0.5)	442.20	±0.84	702.5	0.50
euh sQ	0.1	329	24.3	3.4	2.1	1.6	0.04	117	0.06	0.07168	(0.5)	1.2943	(3.9)	0.1310	(3.5)	446.28	±2.26	843.2	0.81
euh sX	0.1	213	68.6	3.7	1.2	3.0	0.40	200	0.12	0.30308	(0.4)	4.3627	(2.8)	0.1044	(2.5)	1706.58	±6.70	1705.3	0.65

Notes: sample: euh=euhedral, equant; elong=elongate euhedral; s_=single grain; _gr multiple grains.
Weight: represents estimated weight after first step of CATIMS zircon dissolution and is only approximate. U and Pb concentrations are based on this weight and are useful for internal comparisons only. Picograms (pg) sample and common Pb from the second dissolution step are measured directly however, and are accurate. sample Pb: sample Pb (radiogenic + initial) corrected for laboratory blank
cPb: total common Pb. All was assigned to laboratory blank.
Pb*/Pbc: radiogenic Pb to total common Pb (blank + initial)
Corrected atomic ratios: $^{206}Pb/^{204}Pb$ corrected for mass discrimination and tracer, all others corrected for blank, mass discrimination, tracer and initial Pb, values in parentheses are 2 sigma errors in percent.
Th = 206Pb/238U and 207Pb/206Pb ratios and dates corrected for Th disequilibrium assuming Th/U magma of 2.2.
Rho: $^{206}Pb/^{238}U$ vs $^{207}Pb/^{235}U$ error correlation coefficient

Zircon dissolution and chemistry were adapted from methods developed by Krogh (1973), Parrish et al. (1987) and Mattinson (2005). All zircons were chemically abraded (CATIMS). Final dissolutions were spiked with a mixed $^{205}Pb/^{233}U/^{235}U$ tracer (ET535). Pb and UO2 from zircons were loaded onto single rhenium filaments with silica gel without any ion exchange cleanup; isotopic compositions were measured in single Daly-photomultiplier mode on a Micromass Sector 54 thermal ionization mass spectrometer at the University of Wyoming. Mass discrimination for Pb was 0.245±0.10 %/amu for Daly analyses based on replicate analyses of NIST SRM 981. U fractionation was determined internally during each run. Measured procedural blanks ranged from 2 to 0.38 pg Pb during the course of the study. U blanks were consistently less than 0.1 pg. Isotopic composition of the Pb blank was measured as 18.649±0.403, 15.540±0.48, and 37.804±1.69 for 206/204, 207/204 and 208/204, respectively. Concordia coordinates, intercepts, uncertainties and Concordia Ages were calculated using PBMacDAT and ISOPLOT programs (based on Ludwig 1988,

1991, 1998); $^{206}Pb/^{238}U$ and $^{207}Pb/^{206}Pb$ ratios and dates corrected for Th disequilibrium assuming Th/U magma of 2.2 following Schärer (1984).
The decay constants used by PBMacDAT are those recommended by the I.U.G.S. Subcommission on
Geochronology (Steiger and Jäger, 1977): 0.155125 x 10^{-9}/yr for ^{238}U, 0.98485 x 10^{-9}/yr for ^{235}U and present-day
$^{238}U/^{235}U$ = 137.88.

Table C2 CATIMS U-Pb detrital zircon data

								Corrected atomic ratios												
	Weight	U	sample Pb	cPb	Pb*	Th	206Pb	208Pb	206Pb/238UTh		207Pb/235U		207Pb/206PbTh		206/238Th		207/235	207/206Th	Rho
Sample	(µg)	(ppm)	(ppm)	(pg)	(pg)	Pbc	U	204Pb	206Pb	(rad.)	%err	(rad.)	%err	(rad.)	%err	Age (Ma)	err	Age (Ma)	Age (Ma)	
RD0814-035 volcanic tuff					*mix of detrital dates despite euhedral morphologies*															
euh sA	0.11	133	2.2	0.2	2.6	0.1	0.70	23	0.37	0.01147	(14.5)	0.1269	(151.2)	0.0802	(138.4)	73.52	±10.63	121.3	1201.9	0.90
elong sC	0.05	2694	42.0	1.9	1.6	1.2	1.05	79	0.35	0.01259	(1.0)	0.0861	(16.6)	0.0496	(15.7)	80.66	±0.81	83.9	176.3	0.89
euh sB	0.14	1775	29.0	4.1	1.1	3.6	0.50	237	0.16	0.01550	(0.3)	0.1042	(4.5)	0.0487	(4.3)	99.15	±0.30	100.6	133.4	0.81
elong sD	0.30	342	10.0	3.0	1.5	2.0	1.19	119	0.39	0.02318	(0.6)	0.1596	(10.0)	0.0499	(9.5)	147.75	±0.92	150.4	190.4	0.88
RD0814-037 volcanic tuff					*mix of detrital dates despite euhedral morphologies*															
elong sC	0.22	1195	17.8	3.9	2.2	1.7	0.25	131	0.08	0.01520	(0.5)	0.1036	(9.0)	0.0494	(8.6)	97.28	±0.54	100.1	166.9	0.88
euh sA	0.09	211	26.2	2.4	1.8	1.3	0.76	84	0.40	0.09636	(1.0)	0.9518	(11.2)	0.0716	(10.3)	593.02	±6.09	679.0	974.6	0.86
euh sB	0.08	61	8.2	0.7	0.8	0.8	1.19	59	0.34	0.10152	(1.5)	0.8292	(20.1)	0.0592	(18.8)	623.33	±9.07	613.2	574.5	0.89
elong sD	0.18	201	24.8	4.5	0.8	5.4	0.43	315	0.24	0.10648	(0.3)	1.1573	(2.0)	0.0788	(1.9)	652.29	±1.77	780.7	1167.1	0.70
RD0814-041 volcanic tuff					*mix of detrital dates despite euhedral morphologies*															
ash sC	0.14	427	24.3	3.3	2.6	1.2	0.34	102	0.06	0.05946	(1.3)	0.4139	(14.6)	0.0505	(13.4)	372.33	±4.78	351.7	218.0	0.89
euh sA	1.13	70	4.5	5.1	1.9	2.7	0.26	193	0.09	0.06579	(0.6)	0.5051	(6.2)	0.0557	(5.7)	410.77	±2.48	415.2	440.4	0.87
ash sD	0.05	731	54.3	2.8	0.8	3.4	0.12	252	0.04	0.07895	(0.6)	0.6184	(5.7)	0.0568	(5.3)	489.88	±2.72	488.9	483.8	0.75
euh sB	1.13	105	26.5	29.8	0.7	43.5	0.31	2762	0.09	0.24859	(0.2)	3.0931	(0.3)	0.0902	(0.2)	1431.21	±2.32	1431.0	1429.7	0.65

Notes: sample: euh=equant, euhedral; ash=ash-fall zircon characteristics, tips and bubble tracks; elong=elongate, ash-fall morph; s_=single grain.
Weight: represents estimated weight after first step of CATIMS zircon dissolution and is only approximate. U and Pb concentrations are based on this weight and are useful for internal comparisons only. Picograms (pg) sample and common Pb from the second dissolution step are measured directly, however and are accurate. sample Pb: sample Pb (radiogenic + initial) corrected for laboratory blank
cPb: total common Pb. All was assigned to laboratory
blank. Pb*/Pbc: radiogenic Pb to total common Pb
(blank + initial)
Corrected atomic ratios: $^{206}Pb/^{204}Pb$ corrected for mass discrimination and tracer, all others corrected for blank, mass discrimination, tracer and initial Pb, values in parentheses are 2 sigma errors in percent.
Th = 206Pb/238U and 207Pb/206Pb ratios and dates corrected for Th disequilibrium assuming Th/U magma of 2.2.
Rho: $^{206}Pb/^{238}U$ vs $^{207}Pb/^{235}U$ error correlation coefficient

Zircon dissolution and chemistry were adapted from methods developed by Krogh (1973), Parrish et al. (1987) and Mattinson (2005). All zircons were chemically abraded (CATIMS). Final dissolutions were spiked with a mixed $^{205}Pb/^{233}U/^{235}U$ tracer (ET535). Pb and UO2 from zircons were loaded onto single rhenium filaments with silica gel without any ion exchange cleanup; isotopic compositions were measured in single Daly-photomultiplier mode on a Micromass Sector 54 thermal ionization mass spectrometer at the University of Wyoming. Mass discrimination for Pb was 0.245±0.10 %/amu for Daly analyses based on replicate analyses of NIST SRM 981. U fractionation was determined internally during each run. Measured procedural blanks ranged from 2 to 0.38 pg Pb during the course of the study. U blanks were consistently less than 0.1 pg. Isotopic composition of the Pb blank was measured as 18.649±0.403, 15.540±0.48, and 37.804±1.69 for 206/204, 207/204 and 208/204, respectively. Concordia coordinates, intercepts, uncertainties and Cooncrdia Ages were calculated using PBMacDAT and ISOPLOT programs (based on Ludwig 1988, 1991, 1998); $^{206}Pb/^{238}U$ and $^{207}Pb/^{206}Pb$ ratios and dates corrected for Th disequilibrium assuming Th/U magma of 2.2 following Schärer (1984). The decay constants used by PBMacDAT are those recommended by the I.U.G.S. Subcommission on Geochronology: 0.155125 x 10^{-9}/yr for ^{238}U, 0.98485 x 10^{-9}/yr for ^{235}U and present-day $^{238}U/^{235}U$ = 137.88.

Supplement 3 References:

Black, L.P., Kamo, S.L., Allen, C.M., Davis, D.W., Aleinikoff, J.N., Valley, 742 J.W., Mudil, R., Campbell, I.H., Korsch, R.J., Williams, I.S., and Foudoulis, C., 2004, Improved $^{206}Pb/^{238}U$ microprobe geochronology by the monitoring of a trace-element-related matrix effect; SHRIMP, ID-TIMS, ELA-ICPMS and oxygen isotope documentation for a series of zircon standards: Chemical Geology, v. 205, p. 115–140, 746 https://doi.org/10.1016/j.chemgeo.2004.01.003.

Gehrels, G., 2012, Detrital zircon U-Pb geochronology: Current methods and new opportunities, *in* Busby, C., and Azor, A., eds., Tectonics of Sedimentary Basins: Recent Advances: Wiley-Blackwell Publishing, p. 45–62, https://doi.org/10.1002/9781444347166.ch2.

Hu, Z., Gao, S., Liu, Y., Hu, S., Chen, H., and Yuan, H., 2008, Single enhancement in laser ablation ICP-MS by addition of nitrogen in the central channel gas: Journal of Analytical Atomic Spectrometry, v. 23, p. 1093–1101, https://doi.org/10.1039/b804760j.

Krogh, T.E., 1973, A low-contamination method for hydrothermal decomposition of zircon and extraction of U and Pb for isotopic age determinations: Geochimica et Cosmochimica Acta, v. 37, p. 485–494.

Ludwig, K.R., 1988, PBDAT for MS-DOS, a computer program for IBM-PC compatibles for processing raw Pb-U-Th isotope data, version 1.24: U.S. Geological Survey, Open-File Report 88-542, 32 pp.

Ludwig, K.R., 1991, ISOPLOT for MS-DOS, a plotting and regression program for radiogenic-isotope data, for IBM-PC compatible computers, version 2.75: U.S. Geological Survey, Open-File Report 91-445, 45 pp.

Ludwig, K. R. (1998). On the treatment of concordant uranium-lead ages. Geochimica et Cosmochimica Acta, 62(4), 665-676.

Ludwig, K.R., 2012, Isoplot 3.75—A geochronological toolkit for Microsoft Excel: Berkley Geochronology Center Special Publication, v. 5, 75 p.

Paces, J.B., and Miller, J.D., Jr., 1993, Precise U-Pb ages of Duluth Complex and related mafic intrusions, northeastern Minnesota Geochronological insights to physical, petrogenetic, paleomagnetic and tectono-magmatic processes associated with the 1.1 Ga Midcontinent rift system: Journal of Geophysical Research, v. 98, no. B8, p. 13,997–14,013, https://doi.org/10.1029/93JB01159.

Parrish, R.R., Roddick, J.C., Loveridge, W.D., and Sullivan, R.D., l987, Uranium-lead analytical techniques at the geochronology laboratory, Geological Survey of Canada, *in* Radiogenic age and isotopic studies, Report 1: Geological Survey of Canada Paper 87-2, p. 3–7.

Paton, C., Hellstrom, J., Paul, B., Woodhead, J., and Hergt, J., 2011, Iolite: freeware for the visualization and processing of mass spectrometric data: Journal of Analytical Atomic Spectrometry, v. 26, p. 2508–2518, https://doi.org/10.1039/c1ja10172b.

Schärer, U., 1984, The effect of initial ^{230}Th equilibrium on young U-Pb ages: the Makula case, Himalaya. Earth and Planetary Science Letters, v.67, p. 191-204.

Schmitz, M.D., and Bowring, S.A., 2001, U-Pb zircon and titanite systematics of the Fish Canyon Tuff: An assessment of high-precision U-Pb geochronology and its application to young volcanic rocks: Geochimica et Cosmochimica Acta, v. 65, p. 2571–2587, https://doi.org/10.1016/S0016-7037(01)00616-0.

Sláma, J., Košler, J., Condon, D.J., Crowley, J.L., Gerdes, A., Hanchar, J.M., Horstwood, M.S.A., Morris, G.A., Nasdala, L., Norberg, N., Schaltegger, U., Schoene, B., Tubrett, M.N., and Whitehouse, M.J., 2008, Plešovice zircon—A new natural reference material for U-Pb and Hf isotopic microanalysis: Chemical Geology, v. 249, p. 1–35, https://doi.org/10.1016/j.chemgeo.2007.11.005.

Stacey, J.S. and Kramers, J.D., 1975, Approximation of terrestrial lead isotope evolution by a two-stage model: Earth and Planetary Science Letters, v. 26, p. 207–221.

Steiger, R.H. and Jäger, E., 1977, Subcommission on geochronology: convention on the use of decay constants in geo- and cosmochronology: Earth and Planetary Science Letters, v. 36, p. 359–362.